Applied Physics Letters

P-type $In_xGa_{1-x}N$ semibulk templates (0.02 < x < 0.16) with room temperature hole concentration of mid-10^{19} cm^{-3} and device quality surface morphology

Cite as: Appl. Phys. Lett. **119**, 122101 (2021); https://doi.org/10.1063/5.0065194
Submitted: 30 July 2021 • Accepted: 03 September 2021 • Published Online: 20 September 2021

Evyn L. Routh, Mostafa Abdelhamid, Peter Colter, et al.

AIP Publishing

Applied Physics Letters ARTICLE scitation.org/journal/apl

P-type $In_xGa_{1-x}N$ semibulk templates ($0.02 < x < 0.16$) with room temperature hole concentration of mid-10^{19} cm^{-3} and device quality surface morphology

Cite as: Appl. Phys. Lett. **119**, 122101 (2021); doi: 10.1063/5.0065194
Submitted: 30 July 2021 · Accepted: 3 September 2021 ·
Published Online: 20 September 2021

View Online Export Citation CrossMark

Evyn L. Routh,[1,a)] Mostafa Abdelhamid,[2] Peter Colter,[2] N. A. El-Masry,[1,3] and S. M. Bedair[2]

AFFILIATIONS

[1]Department of Materials Science & Engineering, North Carolina State University, Raleigh, North Carolina 27695, USA
[2]Department of Electrical & Computer Engineering, North Carolina State University, Raleigh, North Carolina 27695, USA
[3]National Science Foundation, Alexandria, Virginia 22314, USA

[a)]Author to whom correspondence should be addressed: ellee2@ncsu.edu

ABSTRACT

Using the semibulk approach, p-$In_xGa_{1-x}N$ semibulk (p-SB) templates were grown with an indium content ranging from 2.4% to 15.2% via metalorganic chemical vapor deposition. When compared to optimized bulk p-GaN, the hole concentration in p-SB with an In content of ~15.2% increased by two orders of magnitude from 5.22×10^{17} to 5.28×10^{19} cm^{-3}. The resistivity and mobility of the templates decreased gradually from 3.13 $\Omega \cdot cm$ and 3.82 $cm^2/V\,s$ for p-GaN to 0.24 $\Omega \cdot cm$ and 0.48 $cm^2/V\,s$ for p-SB with an In content of 15.2%. Temperature dependent Hall measurements were conducted to estimate the activation energy of the p-SB template. The p-SB with the In content of ~15.2% is estimated to have an activation energy of 29 meV. These heavily doped p-SB templates have comparable material qualities to that of GaN. The atomic force microscopy height retraces of p-SB films show device quality surface morphology, with root mean square roughness ranging from 2.53 to 4.84 nm. The current results can impact the performances of several nitride-based devices, such as laser diodes, LEDs, solar cells, and photodetectors.

The p-doping of III-nitride materials grown via metalorganic chemical vapor deposition (MOCVD) has been an ongoing challenge in the nitrides community. By utilizing Si as an n-type dopant in GaN, electron concentrations can reach ranges in 10^{19} cm^{-3}.[1] However, p-type doping of MOCVD-grown GaN is two orders of magnitude lower in the 10^{17} cm^{-3} range.[1,2] This asymmetric doping profile within a device can be problematic, as it can result in electron leakage, leading to droop and, thus, decreased performance of long wavelength nitride-based LEDs.[3] In addition, high p-type doping approaching mid-10^{19} cm^{-3} is necessary for utilization of tunnel junctions in InGaN based solar cells. Also high p-type doping will reduce contact resistance for laser diodes with high injection current densities. In LEDs, high p-type doping is used in a lateral current spreading layer to achieve uniform light emission across the device.[4] Therefore, it is advantageous to increase the carrier concentration of MOCVD-grown p-type nitrides. It should be noted that p-GaN grown via molecular beam epitaxy (MBE) and pulsed sputtering deposition (PSD) has achieved hole concentrations in the 10^{18}–10^{19} cm^{-3} range.[5,6] However, the current work reports on hole concentrations as high as 5.28×10^{19} cm^{-3} in MOCVD-grown InGaN.

The challenges of p-type doping are due to several reasons. The only shallow acceptor known for GaN is Mg, which has a high activation energy on the experimental range of 124–230 meV in GaN,[1,7] much higher than the activation energy of Si (~20 meV).[8] In addition, Mg doping of GaN in MOCVD systems suffers from passivation, due to the formation of an Mg–H complex from the free hydrogen as a result of NH_3 decomposition necessary for a nitrogen precursor in GaN films. Thermal annealing[9,10] can aid in reversing this passivation by breaking the Mg–H bond, but even then, not all holes are thermally activated. In addition, too high of a doping concentration during growth can result in self-compensation, from the nitrogen vacancy (V_N) and Mg acceptor interaction,[11] as well as sensitivity to other defects, such as carbon impurities on nitrogen sites.[12] It should also be mentioned that the higher temperatures (upward of 950–1000 °C) necessary to achieve quality p-GaN by MOCVD can degrade the underlying InGaN/GaN quantum well (QW) active region;[13] thus, the lower growth temperature necessary for p-InGaN growth results in a higher quality material in the active region.

The bulk InGaN alloy shows promise for p-type needs of nitride-based devices, as shown by Kumakura *et al.*[14] Others have shown an increase in the hole concentration by using bulk InGaN as the p-type material, showing a hole concentration of mid-10^{18} cm^{-3} as a result of the reduced activation energy of Mg in the ternary alloy.[15] However, bulk InGaN is very rough and suffers from defects, such as formation of V-pits, stacking faults, high dislocation densities, indium inclusions,[16–18] and, thus, does not have adequate material quality for usage in devices. We are not aware of any device structures yet that use bulk grown p-InGaN.

In this report, we demonstrate that the usage of our semibulk low growth temperature approach for Mg doped In_xGa_{1-x} N films, reaching the carrier concentration of 5.28×10^{19} cm^{-3} with device quality surface morphology; this approach can offer solutions to the problems created due to the low hole concentration achieved in Mg doped GaN. It can also be used as templates for n on p solar cells and photodetectors to improve minority carrier collection by having the piezoelectric (PZ) field due to strain in the QW in the same direction as the junction built-in field.

All samples were grown via MOCVD with trimethyl-gallium (TMGa) and trimethyl-indium (TMIn) precursors with hydrogen and nitrogen as carrier gases and ammonia (NH_3) as a nitrogen source. Bis-(cyclopentadienyl)-magnesium (CP_2Mg) was used as the p-type dopant source. All samples in this study were grown at the same Mg doping concentration with a 18.15 nmol/min flow. The Mg concentration in p-GaN was estimated to be 4.2×10^{19} cm^{-3}, as measured by time-of-flight secondary-ion mass-spectrometry (ToF-SIMS). Samples were grown on c-plane sapphire substrates employing a low temperature GaN buffer followed by 1.8 μm thick undoped-GaN and then by the p-semibulk. The semibulk, as described elsewhere,[19,20] was grown with a GaN interlayer thickness of 1–2 nm. From TEM studies, we have observed that the semibulk (SB) templates relax by the formations of V-pits rather than misfit dislocations.[21] The GaN interlayer refills these pits to render a smooth surface. In the current study, the period of the SB is the sum of the InGaN and GaN interlayer films. Five samples are studied, denoted as samples A–E. Sample A, an optimized p-type GaN, was grown totaling a thickness of 0.96 μm. For sample B, the $In_xGa_{1-x}N$ layer in each period was ∼18 nm thick with a total thickness of 0.36 μm. For samples C and D, the $In_xGa_{1-x}N$ thickness was ∼28 nm thick in each period, each with a total thickness of 0.36 and 0.50 μm, respectively. Finally, sample E had an InGaN thickness of ∼30 nm and a total thickness of 0.38 μm. The periods present for samples B–E are varied. The total thickness was verified via interferometry and the periodicity via x-ray diffraction (XRD). A schematic of samples B–E is shown in Fig. 1(a). The In content was controlled by the growth temperature and verified by XRD.

Samples were then annealed at 750 °C in a nitrogen environment for 20 min to thermally activate the carriers present in the semibulk. Photoluminescence (PL) spectra were taken of each sample using a 325 nm HeCd laser. X-ray diffraction (XRD) of the (00.4) reflection was utilized to determine an estimate of the In content of films. Hall measurements in van der Pauw orientation were employed for electrical measurements. Au/Ni contacts were used for the p-SB and p-GaN contacts to ensure the Ohmic behavior of the electrical measurements.[22] Hall measurements with varied temperature were used to determine the activation energy of holes in samples. Samples A, B, and D were measured at a temperature range of 0–170 °C in a thermally insulating environment. Sample E was measured on a range of –115 to 20 °C. All Hall measurements were taken using a 0.6 T magnetic field.

XRD measurements were used to determine an effective In content, x_{eff}. We define x_{eff} as an effective In content or indium content present taking film relaxation into account, as it is important to note that XRD peak separation is an over-estimation of the true In content in relaxed InGaN films. As seen in Ref. 15 by Kumakura *et al.*, using XRD peak separation with an assumption of full relaxation can lead to an over-estimation by 20% and higher.[15,23] x_{eff} for a given sample depends on both the In content from XRD and the total SB thickness. As described in Abdelhamid *et al.*,[19] the extent at which the semibulk is relaxed in the growth direction cannot be easily determined using traditional techniques; thus, we rely on our previous determination of strain-relaxation in our SB to deduce x_{eff}. The SB sample in the current study results in relaxation in the range of 60%–80%. For sample B, a 20-period sample with an 18 nm thick period, the relaxation can be assumed to be similar to previous SBs of similar thickness and periodicity at 60%.[19] For sample C, an increased period of 28 nm can be assumed to give an additional relaxation of 70%. Finally, sample D has

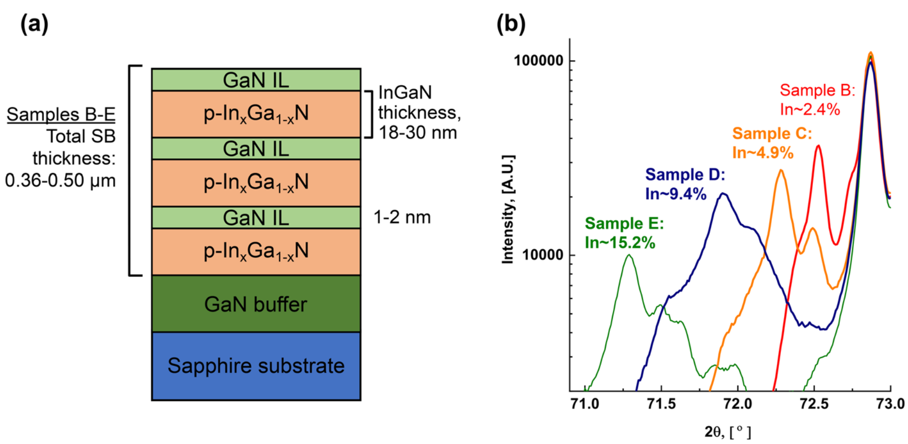

FIG. 1. The schematic of (a) $In_xGa_{1-x}N$ semibulk (SB) samples B–E grown on a low temperature GaN buffer on sapphire. (b) The (00.4) XRD reflection of samples B–E, with an effective In content, x_{eff}.

a larger period of 28 nm, and a larger total thickness, giving an assumption of 80% relaxation; sample E is also assumed to be at 80% relaxation due to the increased indium content in the film. Using Vegard's law, the In content was determined by the peak separation between the $In_xGa_{1-x}N$ peak and the GaN peak and then the relaxation estimations applied to determine the estimated effective indium content x_{eff} in each SB, as noted in Fig. 1(b). The measured In content from XRD for samples B–E was 4%, 7%, 11.7%, and 19%, respectively. Applying the above discussion of relaxation, the effective In content, x_{eff}, for samples B–E is estimated to be 2.4%, 4.9%, 9.4%, and 15.2%, respectively.

As shown in Fig. 2, the electrical characteristics of films showed a dependency on the In content. As seen in Fig. 2(a), the room temperature hole concentration increased with the increasing In content. The hole concentration of sample A (bulk p-GaN) was measured to be 5.22×10^{17} cm^{-3}. For samples B–E, the hole concentrations at room temperature were measured to be 1.39×10^{18}, 2.63×10^{18}, 4.66×10^{18}, and 5.28×10^{19} cm^{-3}, increasing by two orders of magnitude for In $\sim$15.2% as compared to bulk p-GaN. This value is of one of the highest reported for InGaN materials grown by MOCVD. Bulk p-InGaN films[14,15,23,24] reported have an order of magnitude lower hole concentration than the current p-SB approach with comparable indium in the InGaN templates. It is possible that these lower hole concentrations in bulk grown InGaN is a result of the high density of defects in the aforementioned reported bulk grown samples. It should also be mentioned that, for comparison, bulk $In_xGa_{1-x}N$ films with x $\sim$ 29% were able to achieve 1×10^{19} cm^{-3};[24] for semibulk growth, the same order of magnitude doping profile can be achieved by a factor of $\sim$3–3.5$\times$ decrease in the In content. Also $In_xGa_{1-x}N$ with x $\sim$ 18% and a hole concentration of 3×10^{19} cm^{-3} grown via molecular beam epitaxy (MBE) was also reported.[25] As seen in Fig. 2(b), the resistivity also decreases as a function of the In content, decreasing from 3.13 to 0.24 $\Omega \cdot$cm at room temperature. The p-type SB also shows low mobility, as seen in Fig. 2(c), as expected in p-type nitride materials, on the range of $\sim$3.8–0.49 cm^2/V s, consistent with other p-type InGaN films.[15,23] The reduction in hole mobility with the increase in hole concentrations and the In content is expected.[15,23] This drop in resistivities in SB templates relative to the GaN p-type by about an order of magnitude is critical for n on p structures grown on the p-type template; it can result in reduced impact on the fill factor in solar cells and photodetectors.

The activation energy of Mg can be estimated by measuring the temperature dependency of the carrier concentration using an Arrhenius relationship.[14,15] Specifically, the charge neutrality equation

$$\frac{p(p+N_D)}{N_A - N_D - p} = \frac{N_v}{g}\exp\left(-\frac{E_A}{k_B T}\right), \tag{1}$$

where p is the hole concentration, N_D is the donor concentration, N_A is the acceptor concentration, N_V is the effective density of states of holes in the valence band, g is the acceptor degeneracy, and E_A is the acceptor activation energy. A degeneracy factor of 4 was used,[26] and N_D was set to 4×10^{17} cm^{-3} for p-GaN. The effective mass of $In_xGa_{1-x}N$ was calculated using Vegard's law,[27] and the values of the hole effective mass for GaN and InN are 1.96 m_0 and 1.67 m_0, respectively.[28] The values of N_A and N_D are expected to increase with the increasing indium content[29] as well as decreasing growth temperature;[30] Indium has been shown to act as a surfactant, enhancing Mg incorporation.[31] Using the measured Mg concentration in p-GaN from SIMS of $N_A = 4.2 \times 10^{19}$ cm^{-3}, the values of N_A for p-$In_xGa_{1-x}N$ were estimated using the percent increase in N_A with an In content from Ref. 29. The acceptor concentration N_A was estimated to be 4.9×10^{19}, 6.8×10^{19}, and 8.4×10^{19} cm^{-3} for In $\sim$2.4%, 9.4%, and 15.2%, respectively. The same relationship was applied to N_D, which was estimated to be 4.7×10^{17}, 6.6×10^{17}, and 8.2×10^{17} cm^{-3} for In $\sim$2.4%, 9.4%, and 15.2%. The relationship of hole concentration vs reciprocal temperature is shown in Fig. 3(a). It is important to note

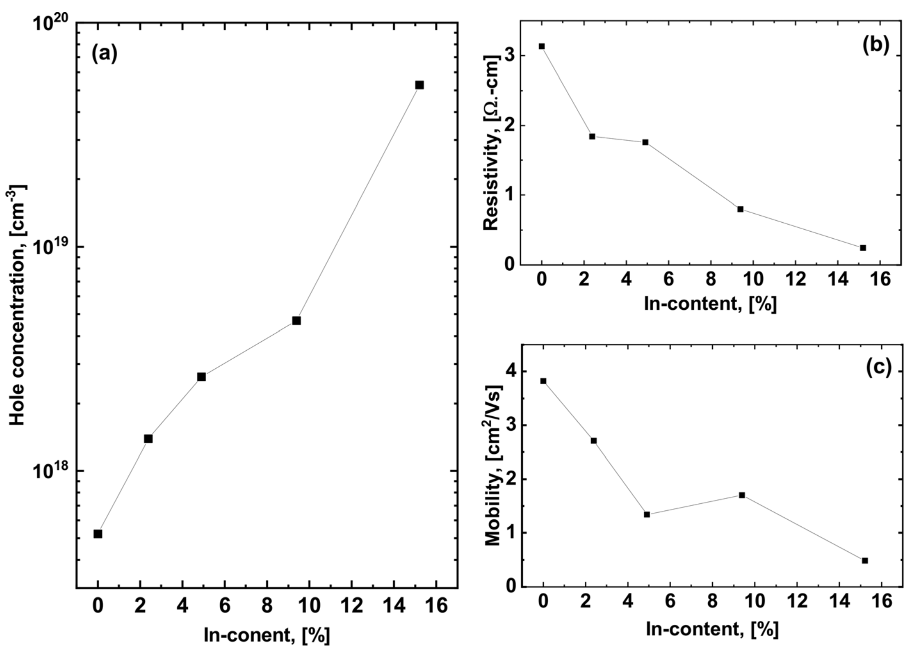

FIG. 2. (a) The hole concentration vs In content at room temperature for the p-doped films, showing a two order of magnitude increase in carriers in SB with In $\sim$15.2%, as compared to bulk p-GaN. (b) Resistivity and (c) mobility of the p-doped films, showing a decrease as a function of the In content.

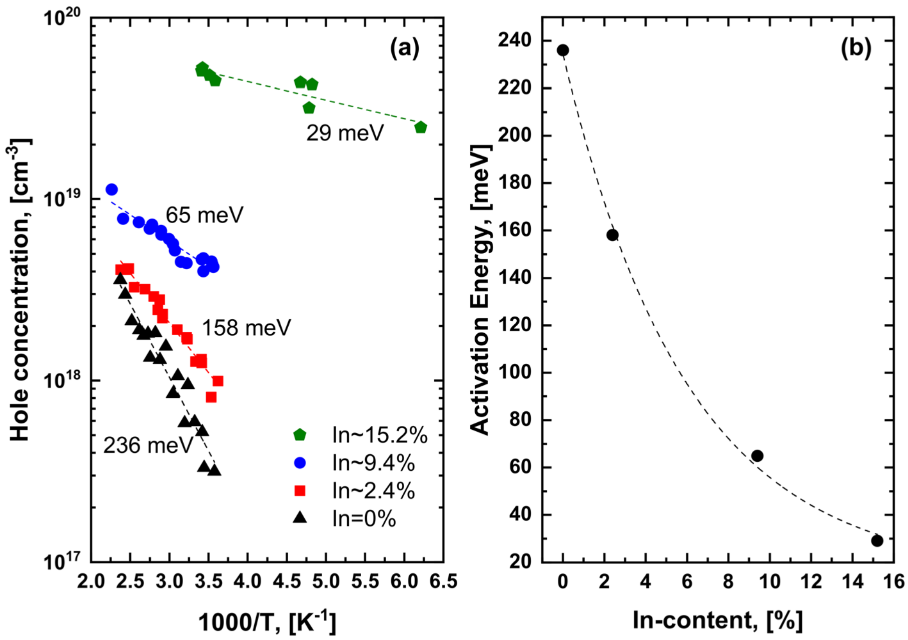

FIG. 3. (a) Hole concentration vs 1000/T obtained via temperature dependent Hall measurements to estimate the activation energy of the p-doped GaN and InGaN SB. (b) The activation energy vs In content; the activation energy of p-GaN was measured to be 236 meV and reduced to 29 meV in a p-SB with In ∼15.2%.

that the dependency of hole concentration on temperature obtained via Hall measurements is used as an estimation of the activation energy. As shown in Fig. 3(b), the resulting estimated activation energy is plotted as a function of an In content. The activation energy is reduced from ∼236 meV in p-GaN to ∼29 meV in an p-SB film with the In content of 15.2%. Previous work on bulk InGaN with In ∼35% showed an activation energy of 43 meV.[23] As was mentioned earlier, Ref. 15 overestimated the In content using XRD techniques in their partially relaxed films. Thus, the low activation energy is consistent with other experimental findings, and it can be deduced that lower activation energies, and, thus, higher carrier concentrations, could be achieved with higher In content SB films.

As shown in Fig. 4, photoluminescence spectra also display a dependency on the In content, as expected. The band edge (BE) emission as denoted by the dashed line "BE" decreases as a function of an In content. The BE emission for Mg-doped GaN was not seen and was dominated by blue luminescence (BL) emission typical of p-GaN films. As noted by the "BL" shaded region, blue luminescence emission related to the Mg^0 doping is observed, and the spacing between the BL region and BE reduces as indium content increases and is measured to be 512, 287, 219, 210, and 141 meV for samples A–E, respectively. Due to the presence of fringing in the BL, the peak position was determined by the peak center of the emission, as marked by arrows in Fig. 4.

The origin of the wide BL region is attributed to several different defects and their interactions in Mg doped GaN and InGaN. Theoretical studies have shown BL from interstitial Mg (Mg_i) and Mg_i interaction with substitutional Mg (Mg_{Ga});[32] this defect complex acts as a deep donor–acceptor pair (D_d–A). This D_d–A transition has also shown to have an In content dependency, with a reduction in the deep donor level and acceptor level with the increasing In content.[15] Thus, a decrease in the BL emission energy and a decrease in the spacing between BL and BE emissions were observed.

As mentioned, p-SB is an excellent alternative to bulk InGaN growth, due to the better material quality and the enhanced surface morphology. We have earlier reported that the SB approach resulted in material quality that is comparable to that of GaN.[20] Device quality surface morphology allows for flexibility in device growth, namely, in multi-junction solar cell growth, n on p solar cells and photodetectors.

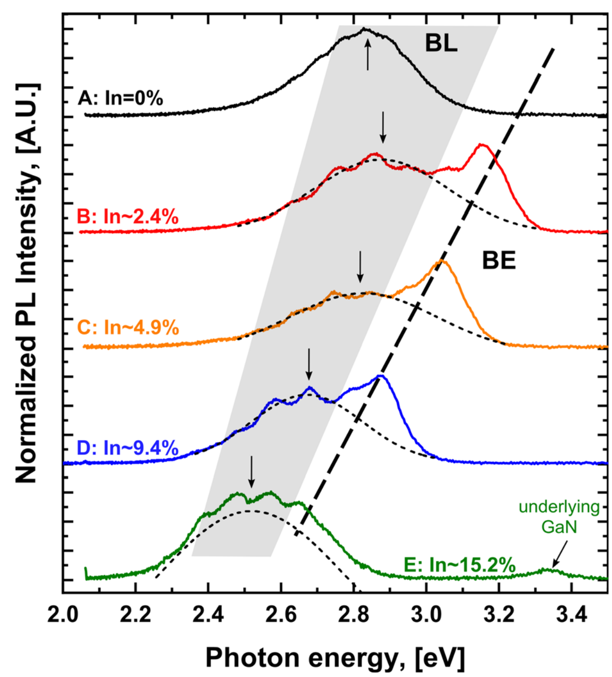

FIG. 4. The photoluminescence of p-doped samples A–E. The band edge emission is denoted by the dashed line BE. Mg-related emissions denoted by the shaded BL region. As the In content increases, the spacing between the BL region and BE decreases.

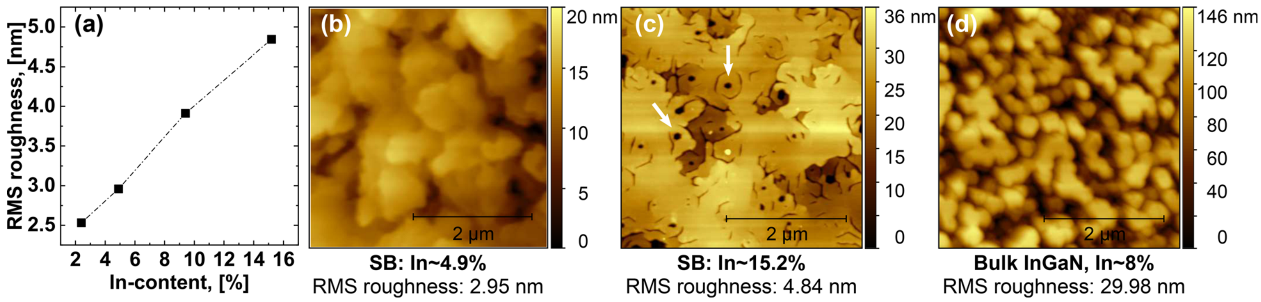

FIG. 5. (a) RMS roughness as measured via AFM vs In content in p-SB films ($4 \times 4\ \mu m)^2$. AFM height retrace of p-SB films, (b) for In ∼4.9% (sample C) and (c) In ∼15.2% (sample E) showing an RMS roughness of 2.53 and 4.84 nm, a drastic improvement when compared to (d) the height retrace of a bulk InGaN sample with In ∼8%, showing RMS roughness of 29.98 nm.

The surface morphology of the p-SB can be seen in the height retrace AFM data in Fig. 5. For p-SB samples B–E, the root mean square (RMS) roughness vs In content is shown in Fig. 5(a). For the In content of 2.4%, 4.9%, 9.4%, and 15.2%, the RMS roughness across ($4 \times 4\ \mu m^2$) was measured to be 2.53, 2.95, 3.91, and 4.84 nm, respectively. AFM height retraces for samples C and E are shown in Figs. 5(b) and 5(c). The surface roughness slightly increases with the increasing In content as expected. As seen in sample E [Fig. 5(c)], In ∼15.2%, pronounced V-pits appear, as indicated by the white arrows evidence of high relaxation in InGaN. For comparison, as seen in Fig. 5(d), bulk InGaN with In ∼8% is significantly rougher, with an RMS roughness of 29.98 nm. Utilizing the semibulk approach allows for a drastic reduction in the surface roughness, for the In content higher than that of bulk.

It should be mentioned that undoped and Si-doped SB templates have surface roughness of about 50% of that of the Mg doped templates for similar In content. They also have dislocation densities (edge- and screw-type) in the low $10^8\ cm^{-2}$ range for same x_{eff} In content.[20] The pit density for samples B–E was measured to be on the range of $1.6–4.7 \times 10^8\ cm^{-2}$. Thus, it seems that the Mg doping does increase the surface roughness slightly.

In SB structures, the GaN interlayers (∼1 nm thick) are under tensile strain due to the lattice mismatch between the relaxing InGaN layers and GaN. A large piezoelectric (PZ) field in GaN layers will result in band bending at the GaN/InGaN interfaces than can, in principal, result in the enhancement of hole concentration, similar to that observed at GaN/AlGaN and InGaN/GaN.[33] However, we are not sure whether the very thin GaN (1–2 nm) can trap these new induced PZ field carriers at these interfaces; the holes may tunnel out through these very strained thin barriers. Also as evident from previous energy dispersive x-ray spectroscopy (EDX)/TEM studies, GaN interlayers are actually InGaN, with low amount of the In content.[21] As mentioned previously, the structures have low residual strain, decreasing the induced PZ field. The parameters will result in a reduction in ΔE_v that will make it less likely that a two-dimensional hole gas (2DHG) is formed at GaN/InGaN interfaces. Thus, even though there might be enhancement in hole concentration, it will not be substantial, as it does take place in every about 20 nm of heavily doped InGaN layers. It is safe to conclude that for $In_xGa_{1-x}N$ SB, the slow and periodic relaxation of the material means that the increased hole concentration is not attributed to band bending and does not expect the generation of a 2DHG, but instead is mainly an intrinsic quality of the material itself. In addition, a polarity inversion from Ga-polar to N-polar is not suspected at this Mg doping concentration, as previous studies have seen polarity inversion at $3 \times 10^{20}\ cm^{-3}$.[34] Previous work on samples grown in our reactor show a polarity inversion at much higher Mg flux than was used in this report.[35]

Another issue in SB templates is the carrier transport, electrons, or holes, across the layers in the growth direction. Si-doped SB with the electron concentration of about $5 \times 10^{18}\ cm^{-3}$ was used as a substrate in several LED structures,[36] and from IV, we did not observe any changes when the n-GaN is replaced by n-SB. The same was observed when the p-GaN was replaced by p-SB with the hole concentration of about $5.5 \times 10^{18}\ cm^{-3}$. Details will be published.

In conclusion, we report increased hole concentration in p-type InGaN templates using the semibulk growth approach. With In ∼15.2%, we report a hole concentration of $5.28 \times 10^{19}\ cm^{-3}$, one of the highest reported carrier concentrations in p-doped GaN and InGaN grown by MOCVD, which was an increase in two orders of magnitude in carrier concentration when compared to p-GaN. The activation energy was estimated using the temperature dependency of hole concentration obtained via Hall measurements. We show a reduction with the increasing In content, with an estimated activation energy of 29 meV in p-SB films with In ∼15.2%. The surface morphology of p-InGaN SB films range from 2.53 to 4.84 nm, suitable for use in devices. This level of hole concentration is sufficient for usage in InGaN tunnel junctions and helps to address the asymmetric doping profiles in InGaN based devices and other applications that can be used to improve InGaN based devices.

The authors would like to acknowledge the Analytical Instrumentation Facility at NCSU for XRD and AFM support. Author N. A. El-Masry would like to acknowledge the National Science Foundation IRD program. The authors thank Dr. Ahmed Shaker (Ain Shams University) for technical discussions. This work is supported by National Science Foundation Grant Nos. ECCS-1407772 and ECCS-1833323. This work was performed in part at the Analytical Instrumentation Facility (AIF) at North Carolina State University, which is supported by the State of North Carolina and the National Science Foundation (Award No. ECCS-2025064). The AIF is a member of the North Carolina Research Triangle

Nanotechnology Network (RTNN), a site in the National Nanotechnology Coordinated Infrastructure (NNCI).

DATA AVAILABILITY

The data that support the findings of this study are available from the corresponding author upon reasonable request.

REFERENCES

[1] K. S. Ramaiah, Y. K. Su, S. J. Chang, F. S. Juang, and C. H. Chen, "Photoluminescence characteristics of Mg-and Si-doped GaN thin films grown by MOCVD technique," J. Cryst. Growth **220**, 405–412 (2000).

[2] X. Chen, K. D. Matthews, D. Hao, W. J. Schaff, and L. F. Eastman, "Growth, fabrication, and characterization of InGaN solar cells," Phys. Status Solidi A **205**, 1103–1105 (2008).

[3] G. Verzellesi, D. Saguatti, M. Meneghini, F. Bertazzi, M. Goano, G. Meneghesso, and E. Zanoni, "Efficiency droop in InGaN/GaN blue light-emitting diodes: Physical mechanisms and remedies," J. Appl. Phys. **114**, 071101 (2013).

[4] A. I. Alhassan, E. C. Young, A. Y. Alyamani, A. Albadri, S. Nakamura, S. P. DenBaars, and J. S. Speck, "Reduced-droop green III-nitride light-emitting diodes utilizing GaN tunnel junction," Appl. Phys. Express **11**, 042101 (2018).

[5] B. Gunning, J. Lowder, M. Moseley, and W. A. Doolittle, "Negligible carrier freeze-out facilitated by impurity band conduction in highly p-type GaN," Appl. Phys. Lett. **101**, 082106 (2012).

[6] T. Fudetani, K. Ueno, A. Kobayashi, and H. Fujioka, "Wide range doping controllability of p-type GaN films prepared via pulsed sputtering," Appl. Phys. Lett. **114**, 032102 (2019).

[7] A. M. Fischer, S. Wang, F. A. Ponce, B. P. Gunning, C. A. M. Fabien, and W. A. Doolittle, "Origin of high hole concentrations in Mg-doped GaN films," Phys. Status Solidi B **254**, 1600668 (2017).

[8] W. Götz, N. M. Johnson, C. Chen, H. Liu, C. Kuo, and W. Imler, "Activation energies of Si donors in GaN," Appl. Phys. Lett. **68**, 3144–3146 (1996).

[9] S. Nakamura, T. Mukai, M. Senoh, N. Iwasa, M. Senoh, A. C. Huang Kuo, S. Jinn Chang, and Y. Kuin Su, "Thermal annealing effects on p-type Mg-doped GaN films," Jpn. J. Appl. Phys., Part 2 **31**, L139–L142 (1992).

[10] F. A. Reboredo and S. T. Pantelides, "Novel defect complexes and their role in the p-type doping of GaN," Phys. Rev. Lett. **82**, 1887 (1999).

[11] H. Obloh, K. H. Bachem, U. Kaufmann, M. Kunzer, M. Maier, A. Ramakrishnan, and P. Schlotter, "Self-compensation in Mg doped p-type GaN grown by MOCVD," J. Cryst. Growth **195**, 270–273 (1998).

[12] T. Narita, K. Tomita, Y. Tokuda, T. Kogiso, M. Horita, and T. Kachi, "The origin of carbon-related carrier compensation in p-type GaN layers grown by MOVPE," J. Appl. Phys. **124**, 215701 (2018).

[13] W. Lee, J. Limb, J. H. Ryou, D. Yoo, T. Chung, and R. D. Dupuis, "Influence of growth temperature and growth rate of p-GaN layers on the characteristics of green light emitting diodes," J. Electron. Mater. **35**, 587–591 (2006).

[14] K. Kumakura, T. Makimoto, and N. Kobayashi, "High hole concentrations in Mg-doped InGaN grown by MOVPE," J. Cryst. Growth **221**, 267–270 (2000).

[15] K. Kumakura, T. Makimoto, and N. Kobayashi, "Mg-acceptor activation mechanism and transport characteristics in p-type InGaN grown by metalorganic vapor phase epitaxy," J. Appl. Phys. **93**, 3370–3375 (2003).

[16] H. K. Cho, J. Y. Lee, G. M. Yang, and C. S. Kim, "Formation mechanism of V defects in the InGaN/GaN multiple quantum wells grown on GaN layers with low threading dislocation density," Appl. Phys. Lett. **79**, 215–217 (2001).

[17] Z. Liliental-Weber, M. Benamara, J. Washburn, J. Z. Domagala, J. Bak-Misiuk, E. L. Piner, J. C. Roberts, and S. M. Bedair, "Relaxation of InGaN thin layers observed by x-ray and transmission electron microscopy studies," J. Electron. Mater. **30**, 439–444 (2001).

[18] D. M. Van Den Broeck, D. Bharrat, Z. Liu, N. A. El-Masry, and S. M. Bedair, "Growth and characterization of high-quality, relaxed $\mathrm{In}y\mathrm{Ga}_{1-}y\mathrm{N}$ templates for optoelectronic applications," J. Electron. Mater. **44**, 4161–4166 (2015).

[19] M. Abdelhamid, J. G. Reynolds, N. A. El-Masry, and S. M. Bedair, "Growth and characterization of $\mathrm{In}x\mathrm{Ga}_{1-}x\mathrm{N}$ ($0 < x < 0.16$) templates for controlled emissions from MQW," J. Cryst. Growth **520**, 18–26 (2019).

[20] E. L. Routh, M. Abdelhamid, N. A. El-Masry, and S. M. Bedair, "Device quality templates of $\mathrm{In}x\mathrm{Ga}_{1-}x\mathrm{N}$ ($x < 0.1$) with defect densities comparable to GaN," Appl. Phys. Lett. **117**, 052103 (2020).

[21] T. B. Eldred, M. Abdelhamid, J. G. Reynolds, N. A. El-Masry, J. M. LeBeau, and S. M. Bedair, "Observing relaxation in device quality InGaN templates by TEM techniques," Appl. Phys. Lett. **116**, 102104 (2020).

[22] Y. C. Lin, S. J. Chang, Y. K. Su, T. Y. Tsai, C. S. Chang, S. C. Shei, C. W. Kuo, and S. C. Chen, "InGaN/GaN light emitting diodes with Ni/Au, Ni/ITO and ITO p-type contacts," Solid-State Electron. **47**, 849–853 (2003).

[23] B. N. Pantha, A. Sedhain, J. Li, J. Y. Lin, and H. X. Jiang, "Electrical and optical properties of p-type InGaN," Appl. Phys. Lett. **95**, 261904 (2009).

[24] C. A. Chang, T. Y. Tang, P. H. Chang, N. C. Chen, and C. T. Liang, "Magnesium doping of In-rich InGaN," Jpn. J. Appl. Phys., Part 1 **46**, 2840–2843 (2007).

[25] J. Pereiro, A. Redondo-Cubero, S. Fernandez-Garrido, C. Rivera, A. Navarro, E. Muñoz, E. Calleja, and R. Gago, "Mg doping of InGaN layers grown by PA-MBE for the fabrication of Schottky barrier photodiodes," J. Phys. D **43**, 335101 (2010).

[26] Z. Liu, X. Yi, Z. Yu, G. Yuan, Y. Liu, J. Wang, J. Li, N. Lu, I. Ferguson, and Y. Zhang, "Impurity resonant states p-type doping in wide-band-gap nitrides," Sci. Rep. **6**, 19537 (2016).

[27] A. Gorai, S. Panda, and D. Biswas, "Advantages of InGaN/InGaN quantum well light emitting diodes: Better electron-hole overlap and stable output," Optik **140**, 665–672 (2017).

[28] Y. C. Yeo, T. C. Chong, and M. F. Li, "Electronic band structures and effective-mass parameters of wurtzite GaN and InN," J. Appl. Phys. **83**, 1429–1436 (1998).

[29] K. Kumakura, T. Makimoto, and N. Kobayashi, "Activation energy and electrical activity of Mg in Mg-doped $\mathrm{In}x\mathrm{Ga}_{1-}x\mathrm{N}$ ($x < 0.2$)," Jpn. J. Appl. Phys., Part 2 **39**, L337–L339 (2000).

[30] E. Haus, I. P. Smorchkova, B. Heying, P. Fini, C. Poblenz, T. Mates, U. K. Mishra, and J. S. Speck, "The role of growth conditions on the p-doping of GaN by plasma-assisted molecular beam epitaxy," J. Cryst. Growth **246**, 55–63 (2002).

[31] Y. Chen, H. Wu, G. Yue, Z. Chen, Z. Zheng, Z. Wu, G. Wang, and H. Jiang, "Enhanced Mg doping efficiency in p-type GaN by indium-surfactant-assisted delta doping method," Appl. Phys. Express **6**, 041001 (2013).

[32] S. Nayak, M. Gupta, U. V. Waghmare, and S. M. Shivaprasad, "Origin of blue luminescence in Mg-doped GaN," Phys. Rev. Appl. **11**, 14027 (2019).

[33] K. Kumakura, T. Makimoto, and N. Kobayashi, "Efficient hole generation above 10^{19} cm^{-3} in Mg-doped in GaN/GaN superlattices at room temperature," Jpn. J. Appl. Phys., Part 2 **39**, L195–L220 (2000).

[34] S. Pezzagna, P. Vennéguès, N. Grandjean, and J. Massies, "Polarity inversion of GaN(0001) by a high Mg doping," J. Cryst. Growth **269**, 249–256 (2004).

[35] A. M. Hosalli, D. M. Van Den Broeck, D. Bharrat, N. A. El-Masry, and S. M. Bedair, "Inversion by metalorganic chemical vapor deposition from N- to Ga-polar gallium nitride and its application to multiple quantum well light-emitting diodes," Appl. Phys. Lett. **103**, 231108 (2013).

[36] M. Abdelhamid, E. L. Routh, and S. M. Bedair, "The dependence of the emission from MQWs on the indium content in the underlying InGaN templates: Experimental and modeling results," Semicond. Sci. Technol. **36**, 035018 (2021).